Thiophene-based water-soluble C_{70} fullerene derivatives as novel antioxidant agents

Margarita Chetyrkina[1], Pavel Umriukhin[2,3*], Elizaveta Ershova[2], Elena Proskurnina[2], Vasilina Sergeeva[2], Ekaterina Savinova[2], Svetlana E. Kostyuk[2], Larisa Kameneva[2], Olga Kraevaya[4], Valeriya Bolshakova[4], Pavel Troshin[4,5], Tatiana Salimova[2], Ivan Rodionov[2], Sergey Kutsev[2], Natalia Veiko[2], and Svetlana V. Kostyuk[2]

ABSTRACT

Fullerenes are one of the most popular nanomaterials, and C_{70} fullerene is the second most common fullerene after C_{60} buckminsterfullerene. Minor modification of fullerenes derivatives can change their biological effects and antioxidant properties. A plethora of water-soluble derivatives can be synthesised based on buckminsterfullerenes. In the present study, we synthesised three water-soluble C_{70} fullerene derivatives with thiophene-based solubilising addends and tested their cytotoxicity and the transcriptional activity of genes, which regulate an oxidative metabolism. Aliphatic chain length in the structure of the solubilising addend of the water-soluble fullerene derivative has been varied, and we revealed that a longer chain resulted in more pronounced antioxidant activity. Thus, the surface modification enhances the antioxidant properties of the compound and changes the nanoparticles impact on the genetic apparatus of the cell. Interestingly, even slight modifications of the functional addend's structure can significantly affect the final cell response. The data obtained can be harnessed to develop novel and efficient medications for the management of ischaemia, stress-related conditions, the prevention of ageing, and the resolution of other practical healthcare challenges.

Keywords:
Antioxidants; Fullerenes; *NRF2*; Reactive oxygen species; Transcription factors

***Corresponding author:**
Pavel Umriukhin,
pavelum@mail.ru

How to cite this article:
Chetyrkina M, Umriukhin P, Ershova E, *et al.* Thiophene-based watersoluble C_{70} fullerene derivatives as novel antioxidant agents. *Biomater Transl.* 2025, 6(3), 359-370.

doi: 10.12336/bmt.24.00064

1. Introduction

Almost 40 years have passed since the remarkable discovery of fullerene by Kroto *et al.*[1] in 1985. The legacy of this finding and other nanomaterials breakthroughs bring the scientific society to the nano world so attractive for application in biomedical tasks.[2-4] Fullerenes are one of the most popular nanomaterials utilised in this field due to their antiviral and antibacterial activity and other promising properties that allow to use them as components of drug delivery systems, as active agents with prospective antioxidant activity, and as photosensitizers for photodynamic therapy.[5-7]

C_{70} fullerene is the second most common fullerene after C_{60} buckminsterfullerene which can be obtained by formal 'insertion' of ten more carbon atoms along the equator of C_{60}. Thus, the molecule takes the form of an elongated spheroid, and the additional carbon 'belt' contains atoms with the maximum chemical activity because of the unpaired electrons.[8-10] While biological effects and mechanisms of action for C_{60} and its water-soluble derivatives are extensively studied, for C_{70} there exists a big gap in the knowledge, and only a small portion of works touched the compound bio-effects. In general, there are three main characteristics which influence impact of fullerenes on various bio-objects: lipophilicity, which determines the membranotropic properties of fullerenes, electron deficiency, which is one of the reasons behind the interaction of fullerene molecule with free active radicals, and the ability in an excited state to transfer the energy to other molecules.[5] Polyoxometalate nanomaterials have emerged as potent agents for quenching reactive oxygen species (ROS),[11] carbon quantum dots have been widely used in biomedical applications owing to their ROS scavenging ability.[12]

Zhou *et al.*[13] had shown that C_{70} modified with L-lysin or β-alanine promoted the protection from a chemotherapy-induced hepatotoxicity and cardiotoxicity on a mice model. The comparison of compounds revealed that fullerene modified with L-lysine was more prospective in terms of ROS scavenging ability – 87% against 49% for β-alanine. The detected effect is most likely associated with the molecules charge[14] and proteins corona surrounding all nanoparticles and affecting nanomaterials penetration into cells.[15] One more study demonstrated an antiviral activity of polycarboxylic derivatives of fullerenes C_{70} is comparable with C_{60}.[16] Decacationic malonate ester C_{70} fullerene [> $M(C_3N_6^+C_3)_2$] was tested as a photosensitizer to induce photokilling in harmful bacteria cells and cancer cells.[17] The results showed that C_{70} is more efficient in terms of ROS production than C_{60} modified in the same way. Looking back, many researchers made multiple attempts to fight coronavirus disease 2019 (COVID-19), and fullerenes C_{70} were also tested for the chance to inhibit the main severe acute respiratory syndrome-related coronavirus 2 (SARS-CoV-2) virus protease.[18] Several works demonstrated an effective scavenging of ROS and antioxidant properties of C_{70}.[19, 20] Based on the abovementioned, the great potential of C_{70} water-soluble fullerenes application in biological systems is obvious, so the next set of studies should shed the light on the mechanisms and probably more beneficial effects.

Possibility to attach functional groups to the fullerene cage via substitution of the chlorine atoms in the chlorofullerenes structure, such as for example $C_{60}Cl_6$ and $C_{70}Cl_8$, allows to obtain a wide range of various fullerene derivatives.[21, 22] At the same time, attachment of excessive number of functionalities to the fullerene cage disrupts the system of the double bonds thus decreasing the ability of the cage to interact with ROS and, as a result, antioxidant properties. Thus, a compromise should be found for the best combination of water-solubility and antioxidant activity.

Extensive studies of biomedical effects of thiophene-based derivatives have been performed as well. Due to the simple heterocyclic system with the well-developed chemical approaches for accurate positioning of functionalities, a big variety of thiophene-based chemical structures have been developed. A review by Roman[23] contains more than 300 different thiophene-based compounds, and their potential antimicrobial activity is extensively discussed. Several other review articles also revealed biological activity of thiophene-based structures.[24,25] Several studies describe the inhibition of carbonic anhydrase I and II targeting carbon dioxide under the treatment with thiophene-based derivatives, so the authors proposed an effective application of the synthesised chemicals for healing of neurological diseases, mountain sickness, glaucoma, and osteoporosis.[26,27] The research conducted by Xu *et al.* revealed that the primary mechanism underlying the action of the thiophene derivative naturally occurring in Echinops grijsii root extracts is based on the production of ROS and the induction of apoptosis in cells.[28] This peculiarity of a natural healing is used in a traditional Chinese medicine for breast, lung and colon cancer treatment. Simulation studies were done to reveal step-by-step reactions of thiophene and its derivatives with ROS, photo-degradation sequence and processes of reactive oxygen generation.[29-31] In addition, antiviral properties have been successfully tested on thiophene-based fullerenes C_{60} and C_{70}. The broad panel of viruses was tested *in vitro* and *in vivo*.[32]

In the present study, we explore the *in vitro* effects of three C_{70} fullerene derivatives bearing thiophene substituents to determine whether the combination of these thiophene radicals with the C_{70} cage yields promising biological outcomes. For that purpose, a standard cytotoxicity assay and tests for intracellular ROS counting were performed with flow-cytometry and fluorescence microscopy. Furthermore, a comprehensive analysis of a wide range of genes and their protein expression patterns associated with ROS was conducted with the aim of detecting molecular alterations in cellular processes. Thus, the present study presents an in-depth examination of three nanosubstances, focusing on their antioxidant properties and their potential use in translational medical applications.

2. Methods

2.1. Synthesis and characterisation of fullerene derivatives

C_{70} fullerene derivatives with thiophene-based solubilising addends were synthesised at the Federal Research Centre for Problems of Chemical Physics and Medicinal Chemistry of RAS (Chernogolovka, Russian Federation) from chlorofullerene $C_{70}Cl_8$. Detailed synthesis and characterisation are described in our previous works.[32,33] Molecular structures of the synthesised compounds are demonstrated in **Figure 1**. As could be seen, the only difference between chemical structures is the length of the aliphatic chains attached to the thiophene heterocycle. Fullerene-based potassium salts can dissociate in water, resulting in the formation of fullerene-based carboxylates and K^+ ions.

2.2. Cell culture

Human embryonic lung fibroblasts (4th passage) were obtained from the Biobank collection of the Research Centre for Medical Genetics. Cells were validated by short tandem repeat profiling profiling and tested negative for mycoplasma. Human embryonic lung fibroblast is a highly sensitive cell line, which is why it is widely used in cytotoxic assays for novel pharmaceuticals, particularly in the context of fullerene research.[34-36]

Cultivation was performed in Petri dishes (Eppendorf, Hamburg. Germany) at standard conditions (37°C, 5% CO_2)

[1]Higher School of Economics, Moscow, Russia; [2]Department of Molecular Biology, Research Centre for Medical Genetics, Moscow, Russia; [3]Department of Normal Physiology, I.M. Sechenov First Moscow State Medical University (Sechenov University), Moscow, Russia; [4]Department of Kinetics and Catalysis, Federal Research Centre for Problems of Chemical Physics and Medicinal Chemistry of RAS, Chernogolovka, Russia; [5]Zhengzhou Research Institute of HIT, Zhengzhou, Henan Province, China

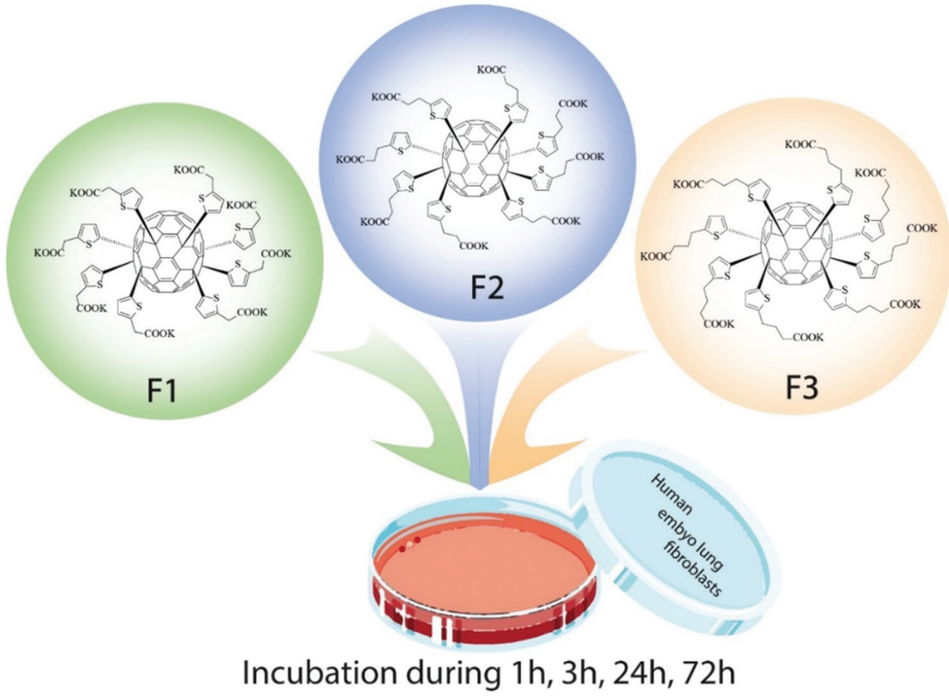

Figure 1. Molecular structures of the tested thiophene-based compounds F1, F2 and F3. Created with ChemSketch software.

in a humidified incubator. DMEM (PanEco, Moscow, Russia) with 10% fetal calf serum (PAA, Vienna, Austria) and addition of 50 U/mL penicillin (PanEco), 50 μg/mL streptomycin (PanEco), 10 mg/mL gentamicin (PanEco) was applied for cell culturing. The media was refreshed every 2–3 days.

In order to assess the effect of fullerenes, the cells were tested at 1, 3, 24, and 72 hours after incubation.

2.3. Cytotoxicity test

The cells were grown in a 96-well plate (Eppendorf) for 72 hours at standard conditions (37°C, 5% CO_2) in a humidified incubator. Cell viability was assessed by the colorimetric 3-(4,5-dimethylthiazol-2-yl)-2,5-diphenyltetrazolium bromide (MTT) test (Biolot, Sankt-Petersburg, Russia). Fluorescence assay was measured with EnSpire Plate Reader (EnSpire Equipment, Turku, Finland) at 550 nm wavelength.

2.4. Assessment of intracellular ROS

Intracellular ROS was detected with 2,7-dichlorodihydrofluorescein diacetate (DCFH-DA) (Molecular Probes/Invitrogen, Carlsbad, CA, USA), which is oxidized by ROS to form fluorescent 2,7-dichlorofluorescein. ROS were detected by two methods – fluorescence microscopy and flow cytometry.

2.4.1. Fluorescence microscopy

Fluorescence microscopy was performed using AxioVert microscope (Carl Zeiss, Oberkochen, Germany). A 3.7% solution of formaldehyde was used for cell fixation, which was applied for 20 minutes at a temperature of 4°C. Subsequently, the cells were subjected to treatment with 0.1% Triton X-100 (PanEco) in a buffered saline solution (PBS; PanEco). The cells were subsequently washed using 1% albumin in PBS.

2.4.2. Flow cytometry

To prepare cells for flow cytometry, cells were firstly treated with Versene (Thermo Fisher Scientific, Waltham, MA, USA) and 0.25% trypsin (Paneco) solution. For cell washing, Dulbecco's modified Eagle medium (DMEM) culture medium and PBS were applied. Paraformaldehyde reagent (Sigma-Aldrich, St. Louis, MO, USA) was employed for subsequent fixation (duration: 10 minutes). Following three rounds of washing, the cells were subjected to a treatment with a 0.1% solution of Triton X-100 in PBS, which lasted for 15 minutes at room temperature. At the last step, cells again were washed three times with 0.5% bovine serum albumin (BSA)–PBS solutions. Flow-cytometry was performed with Partec CyFlow® ML, Germany.

2.5. Assessment of gene and protein expression

The assessment of gene expression was carried out using real-time polymerase chain reaction. Following exposure to fullerenes, RNA was extracted from cells using YellowSolve kits (Klonogen, Moscow, Russia) in accordance with the standard protocol. This was followed by phenol–chloroform extraction and precipitation using chloroform and isopropyl alcohol in a 49:1 ratio. The concentration of RNA was determined using the Quant-iT RiboGreen reagent (MoBiTec, Göttingen, Germany) on an EnSpire plate reader (Finland) with λ_{ex} = 487 nm and λ_{fl} = 524 nm. Reverse transcription was performed using Sileks reagents (Moscow, Russia) following the standard procedure. Polymerase chain reaction was performed using appropriate primers from Synthol (Moscow, Russia) and the intercalating dye SybrGreen from Helicon (Moscow, Russia) on a StepOnePlus apparatus from Applied Biosystems (Waltham, MA, USA). The primer sequences are shown in **Table 1**.

Table 1. Primer sequences

Gene	Primer sequence (5′–3′)
BCL2	Forward: TTTGGAAATCCGACCACTAA Reverse: AAAGAAATGCAAGTGAATGA
CCND1	Forward: TTCGTGGCCTCTAAGATGAAGG Reverse: GAGCAGCTCCATTTGCAGC
CDKN1A	Forward: GGAAGACCATGTGGACCTGT Reverse: ATGCCCAGCACTCTTAGGAA
DKN2	Forward: ATGGAGCCTTCGGCTGACT Reverse: GTAACTATTCGGTGCGTTGGG
BRCA1	Forward: GGCTATCCTCTCAGAGTGACATTTTA Reverse: GCTTTATCAGGTTATGTTGCATGGT
BAX	Forward: CCCGAGAGGTCTTTTTCCGAG Reverse: CCAGCCCATGATGGTTCTGAT
HO1 (HMOX1)	Forward: TCCTGGCTCAGCCTCAAATG Reverse: CGTTAAACACCTCCCTCCCC
LC3	Forward: AACATGAGCGAGTTGGTCAAG Reverse: GCTCGTAGATGTCCGCGAT
NFKB1	Forward: CAGATGGCCCATACCTTCAAAT Reverse: CGGAAACGAAATCCTCTCTGTT
NOX4	Forward: TTGGGGCTAGGATTGTGTCTA Reverse: GAGTGTTCGGCACATGGGTA
NQO	Forward: AGCGAGTGTTCATAGGAGAGT Reverse: GCAGAGAGTACATGGAGCCAC
NRF2	Forward: TCCAGTCAGAAACCAGTGGAT Reverse: GAATGTCTGCGCCAAAAGCTG
SOD1	Forward: AGGGCATCATCAATTTCGAGC Reverse: GCCCACCGTGTTTTCTGGA
TBP (reference)	Forward: GCCCGAAACGCCGAATAT Reverse: CCGTGGTTCGTGGCTCTCTCT

The quantification of protein expression was achieved through the use of flow cytometry, employing specific antibodies on a Cytoflex S (Beckman Coulter's, Indianapolis, IN, USA). The following antibodies were used: CY5.5-NOX4 (Bioss Inc., Woburn, MA, USA, Cat# bs-1091r-cy5-5); *NRF2* pSer40 (Bioss Inc., Cat# bs2013); PE-8OHdG (Santa Cruz Biotechnology, Dallas, TXs, USA, Cat# sc-393871 PE); DyLight488-γH2AX (pSer139) (NovusBio, St. Charles, MO, USA, Cat# nb100-78356G); FITC-*BRCA1*, (NovusBio, Cat#NB100-598F); *LC3* (NovusBio, Cat# NB2220G (DyLight 488)); Ki-67 (NovusBio, Cat# sc-23900 FITC). Incubation lased overnight at 4°C. Secondary mouse anti-rabbit IgG-FITC (Santa Cruz Biotechnology, Cat# sc-2359), incubation lasted 1 hour at room temperature.

2.6. Statistical analysis

The experiments were performed in triplicate. The data are expressed as mean and standard deviation (SD). The significance of differences was analyzed using non-parametric Mann-Whitney *U* criterion. $P < 0.01$ was considered as statistically significant. StatPlus2007 software (AnalystSoft Inc., Alexandria, VA, USA) was used for data analysis.

3. Results

3.1. Cytotoxicity and cell uptake of fullerenes

In order to assess cytotoxicity, we conducted a standard MTT assay for 72 hours of incubation with the fullerenes under investigation. Despite the great potential of various simulations of drugs cytotoxicity and so-called *in silico* methods, there is still an urgent need to test new drugs cytotoxicity in the living systems.[37-39]

To compare the fullerene cytotoxicity, we have found an IC_{50} (inhibitory concentration) value at which 50% of cells are alive compared to the control group without addition of any compound. F1 showed the lowest IC_{50} value of 88 μg/mL (**Figure 2A** – green line), which means that cells are quite sensitive to this fullerene derivative. At the same time, F2 and F3 demonstrated almost similar IC_{50} values – 478 and 451 μg/mL, respectively. Such remarkable difference (5 fold) in a cytotoxic response may be a result of the different dissociation rate of fullerenes in water, a longer aliphatic chain is leading to a slower rate of dissociation.[40] Based on the MTT data, the limiting non-toxic concentration (28 μg/mL) with 90% cell viability for all fullerenes was chosen for the further studies and visualisation. Up to 28 μg/mL concentration the graphs for F1, F2 and F3 have the same profiles as depicted in **Figure 2A**.

All of the tested compounds have an intrinsic fluorescence with a maximum peak in the range of 620–625 nm. Using flow cytometry, we were able to observe the fullerenes penetration into the cells after incubation. It should be noted, that only after 1 hour of incubation the fullerenes were observed inside the cells by flow cytometry and the value was significantly different from the control value for all of the tested structures. After three hours, we observed the peak of fullerene intensity within the cells, while subsequent time points, namely 24 and 72 hours, revealed a reduction in intensity. After 72 hours of incubation, the fluorescence intensity was the same as after 1 hour, which probably means that somehow fullerenes degrade inside cells over time (**Figure 2C**).

The results which have been obtained by flow cytometry were supported by fluorescence microscopy (**Figure 3**). Cells were incubated with the compounds during 1 hour before the visualisation of fullerenes localisation inside the cells. Most of the fullerene molecules were located in the centre of cells around the nuclei, there was no evidence of fullerenes translocation through the nuclear membranes. Almost no fullerenes were observed at the cell periphery, lamellipodia or filopodia. This result allows us to suggest that the diffusion of fullerenes through the cell membrane occurs during several minutes and is thermodynamically beneficial which is also supported by the previous data.[41, 42]

3.2. Intracellular ROS evaluation in fullerenes

ROS are important signalling molecules in cells playing a role in cell proliferation, apoptosis and cell-to-cell crosstalk.[43] On another hand, an excessive synthesis of ROS by cells because of the disruption of the intracellular processes and/or external influences cause cell death or cell damage.[44] Thus, the imbalance of ROS concentration in one or the other side is an indicator of changes in cell metabolism.[45]

Figure 2B presents the findings of an assessment ofROS levels in cells using flow cytometry. ROS concentration in cells was assessed with DCFH-DA method.[46] Non-fluorescent

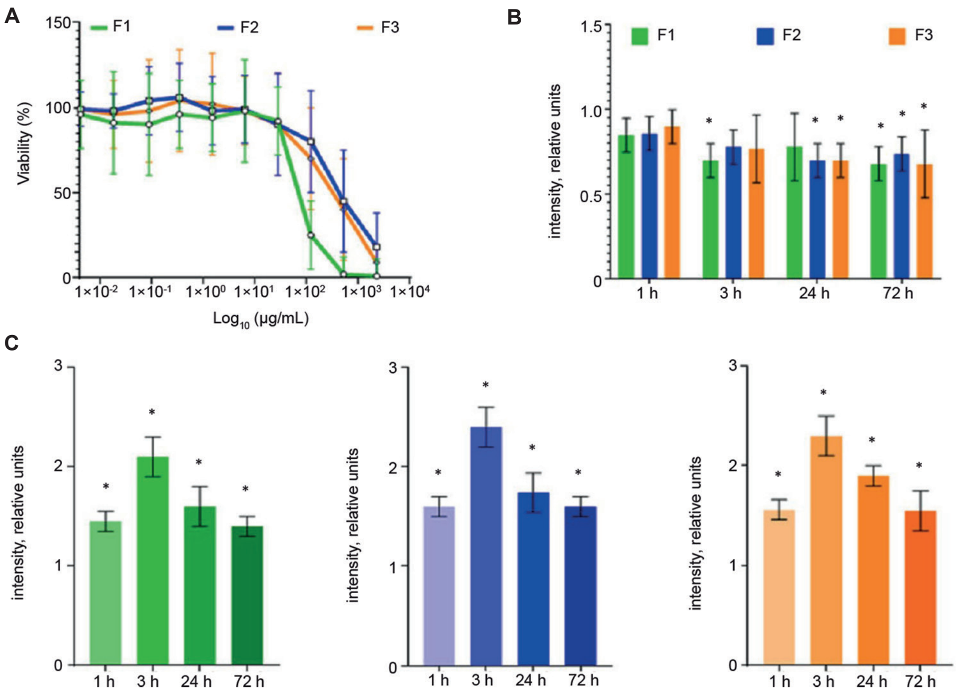

Figure 2. (A) cytotoxicity for fullerenes F1-F3 in human embryonic lung fibroblasts after 72 hours of incubation. (B) Intracellular ROS detection after incubation after 1, 3, 24, and 72 hours. (C) Fluorescent intensity of fullerenes penetrated inside cells. The data are expressed as mean ± SD. $^{*}P < 0.01$, vs. control (non-parametric Mann-Whitney *U* test).

DCFH in the cytoplasm is a highly sensitive marker to ROS and it is oxidised by free radicals to intensely fluorescent 2,7-dichlorofluorescein that could be detected.

The cells were incubated with fullerenes for a period of 72 hours. However, the reaction of the cells was monitored from the start of the incubation period at 1 hour (**Figure 2B**). In general, all the fullerenes tested showed a significant reduction in ROS levels in cells, although the duration of effect development varied. Significant difference compared to the control group was found after 3 hours for fullerene F1, while for fullerenes F2 and F3 the significant reduction in ROS was observed only after 24 hours. This result is supported by our previous MTT data where we revealed a remarkable difference in IC_{50} values – F1 acts more rapidly at lower doses than F2 and F3. Thus, ROS reduction and difference in cell viability probably is a consequence of different bioavailability of fullerenes. After 72 hours all of the tested compounds had shown the significant decrease of ROS in the range of 26-32% that proves the ability of the thiophene-based fullerenes to promote a long-term anti-oxidant effect.

Figure 4 demonstrates ROS generation with the same DCFH-DA method by fluorescence microscopy. Green colour on the second column demonstrates ROS distribution and visualizes “black dots” after fullerenes addition. Red colour on third column indicates fullerenes localisation in cells, “black dots” are red-coloured and filled by fullerenes.

Aside from the revealed antioxidant properties of fullerenes, there is still a probability of ROS generation by fullerenes under light illumination.[47,48] Besides, there is a chance that thiophene-based compounds may act as ROS creators, as was previously shown in some studies.[49,50] Summing up, we propose the presence of two competing processes in human embryonic lung fibroblasts in response to fullerenes treatment – inhibition of ROS generation that was already proved in the previous series of experiments, and ROS production. The last hypothesis should be carefully checked through the assessment of expression of genes and proteins associated with ROS.

3.3. Genes and proteins expression as a response to incubation with fullerenes

Investigation of genes and protein expression was performed at four time points – 1, 3, 24 and 72 hours. In general, the genes and proteins can be divided into two broad categories based on the degree of expression changes (**Table 2**).

The heat maps mentioned that in common, the profile and tendencies are the same for all of the tested fullerenes (**Figure 5**). The highest modification is notable after 24 and 72 hours. For F1 no changes were found after 1 hour, meanwhile for F2 and F3 compounds we were able to register changes in *CCND1* gene expression. *CCND1* gene was activated in cells incubated with F1 only after 3 hours. At that time point, the decrease in NOX4 protein was detected in cells treated with F1. For F2 and F3 after 3 hours we have found several changes in gene/protein expressions – *Nox4*, *NRF2*, and *NRF2*. For F2 we also found an increased level of 8-oxo-guanine (8OxoG), when for F3 *HO1* expression was increased.

Principally, the division into two groups demonstrated in **Table 2** is very similar for the tested fullerenes, and only small deviations are notable. *NOX4, NRF2* and *NRF2* are in the first group with the greatest changes for all of the tested fullerenes.

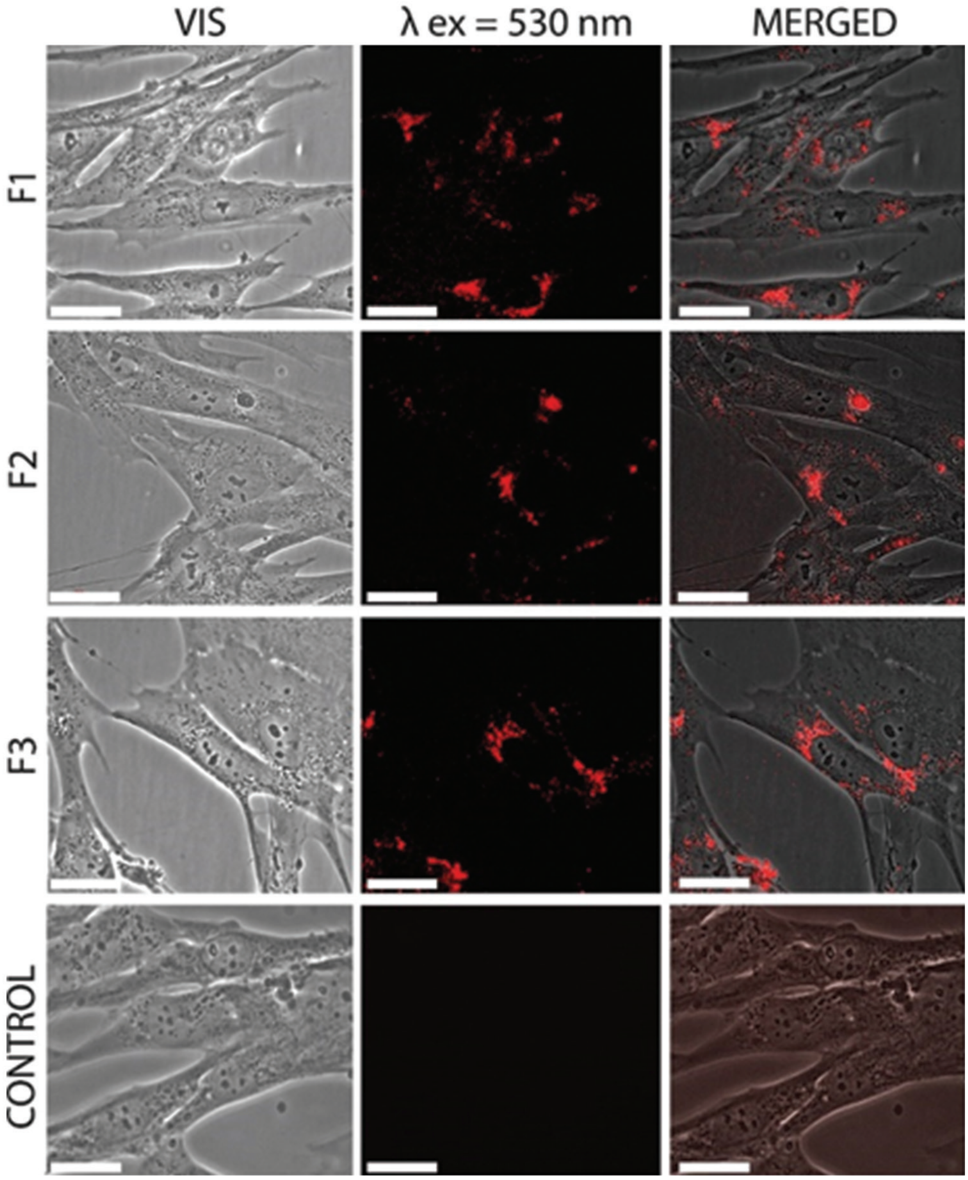

Figure 3. Effect of fullerenes F1–3 on morphology human embryonic lung fibroblasts after 1-hour incubation. Left column visualises optical light microscopy images of cells, the middle column shows the fluorescence photo (fluorescence of the fullerenes inside cells), and the right one demonstrates the merged images. Scale bars: 20 μm.

NOX4 enzyme, one of the crucial NADPH oxidases, which is catalysing the synthesis of hydrogen peroxide and is one of the main sources of ROS in fibroblasts.[51] Thus, the *NOX4* gene and protein activate as a response to stimuli, promoting oxidative stress in cells and inducing fibrosis.[52] As can be observed in **Table 1**, the expression of the *NOX4* gene undergoes a marked increase, whereas the alterations in its protein expression exhibit a lesser degree, resulting in a decrease relative to the baseline level. The time of activation for the *NOX4* gene differs depending on the isoform: for F2 and F3, it is 3 hours; for F1, the level of gene expression becomes active after 24 hours.

To conclude, *NOX4* gene responsible forROS generation, exhibits a rapid activation in fibroblasts in the presence of F2 and F3. Conversely, for F1 a marked increase in the *NOX4* expression occurs only over a period of 24 hours.

Conversely, both the gene and protein expression of the *NRF2* are in the same first category, indicating a highly active response of these elements. NRF2 is a leucine zipper transcription factor, which is known for more than 20 years because of its significant role in antioxidant protection of cells.[53] The primary role of NRF2 is to orchestrate a cellular response to a variety of oxidants.[54] The activation of the *NRF2* gene and the upregulation of its protein expression place these entities in the first group, indicating that the cells have initiated the antioxidant response.

For F1, the expression of the gene and protein is increased after 24 hours in parallel to *NOX4*, so the counteraction of two processes is taking place in the cells. For F2 and F3, a substantial increase is observed after 3 hours, which persists up to 24 hours for both the gene and the protein. Moreover, for F3, there is also a marked shift towards an increase after

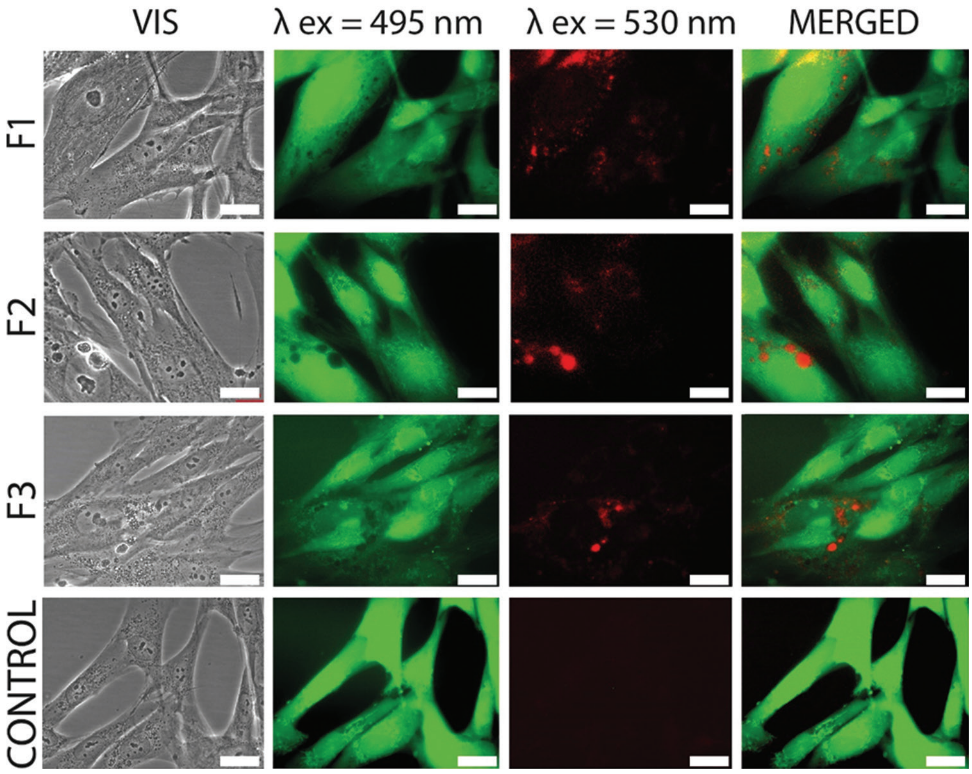

Figure 4. Effect of fullerenes on ROS-scavenging properties in human embryonic lung fibroblasts. Optical microscopy (first column) and fluorescence microscopy (second, third and fourth columns) images of cells incubated with the fullerenes (red) during 25 hours and dye for ROS (DCFH-DA) (green). Second column visualizes the coloring of the cells with dye for ROS, third column shows fluorescence of the fullerenes, the last column demonstrates both fluorescence events. Scale bars: 20 μm.

Table 2. Classification of genes and proteins according to their expression after fullerenes addition

Group	Compound	Gene/protein
1	F1	*NOX4*, *NRF2*, *NRF2*, *HO1*, *NQO*, *BRCA1*, *CCND1*, *CDKN1A*, *LC3*
	F2	*NOX4*, *NRF2*, *NRF2*, *HO1*, *NQO*, *BRCA1*, *CDKN1A*
	F3	*NOX4*, *NRF2*, *NRF2*, *HO1*, *NQO*, *BRCA1*, *CCND1*, *LC3*, *LC3*
2	F1	*NOX4*, *SOD1*, *8OxoG*, *H2Ax*, *CDKN2*, *BCL2/BAX*, *Ki-67*, *LC3*
	F2	*NOX4*, *SOD1*, *8OxoG*, *H2Ax*, *CCND1*, *CDKN2*, *BCL2/BAX*, *Ki-67*, *LC3*, *LC3*
	F3	*NOX4*, *SOD1*, *8OxoG*, *H2Ax*, *CDKN1A*, *CDKN2*, *BCL2/BAX*, *Ki-67*

Notes: Group 1 – changes of expression are higher or equal 50%; and group 2 – expression variability is less than 50% compared to the control value. F1, F2, F3 indices three fullerenes, and their structural formulae are shown in the **Figure 1**. Green means the increased expression, red color meansthe decreased expression; and black means no significant change.

72 hours, indicating the prolonged antioxidant activity of that compound.

Searching for the relation between NOX4 and NRF2, we have found a study where the activation of NRF2 was mediated by NOX4 in cardiac cells.[55] Another study describes how the activation of NRF2 under the action of NOX4 promotes the survival in cancer associated fibroblasts and tumorigenesis.[56] Thus, there is a close correlation between these two genes, and in healthy fibroblasts, their balance should be perfectly harmonious. In our study, we observed a decrease in the expression of the NOX4 protein, which is responsible for regulating the production ofROS, when the *NOX4* gene is upregulated. Therefore, we have ample evidence to suggest that the *NOX4* gene may be involved in the activation of *NRF2* triggered anti-oxidant pathway.

It has been previously demonstrated that *NRF2* initiates the so-called NRF2–ARE pathway, which is responsible for the activation of defence mechanisms in cells and their subsequent protection.[57] Thus, *NRF2* triggers the activation of the *NQO1* gene, which is involved in cellular protection against ROS, leading to a significant alteration in its expression towards an increase. Similarly, *NRF2* enhances the expression of the *HO1* gene.[58] Both *NQO1* and *HO1* serve as markers of cellular modifications aimed at eliminating ROS, representing a crucial aspect of antioxidant activity. These enzymes are classified as belonging to the first group in **Table 2**.[59,60] The *HO1* gene becomes activated at both 24- and 72-hour intervals for all fullerenes. However, an elevated level was also detected after 3 hours in the case of F3 (**Figure 5**). For NQO1 we found a similar response in cells – the increased level of expression after 24 and 72 hours.

Another gene, *SOD1*, was subjected to testing for its expression due to the capacity of superoxide dismutase-1 to metabolise superoxide radicals into molecular oxygen. We have found that in response to the incubation with fullerenes, cells

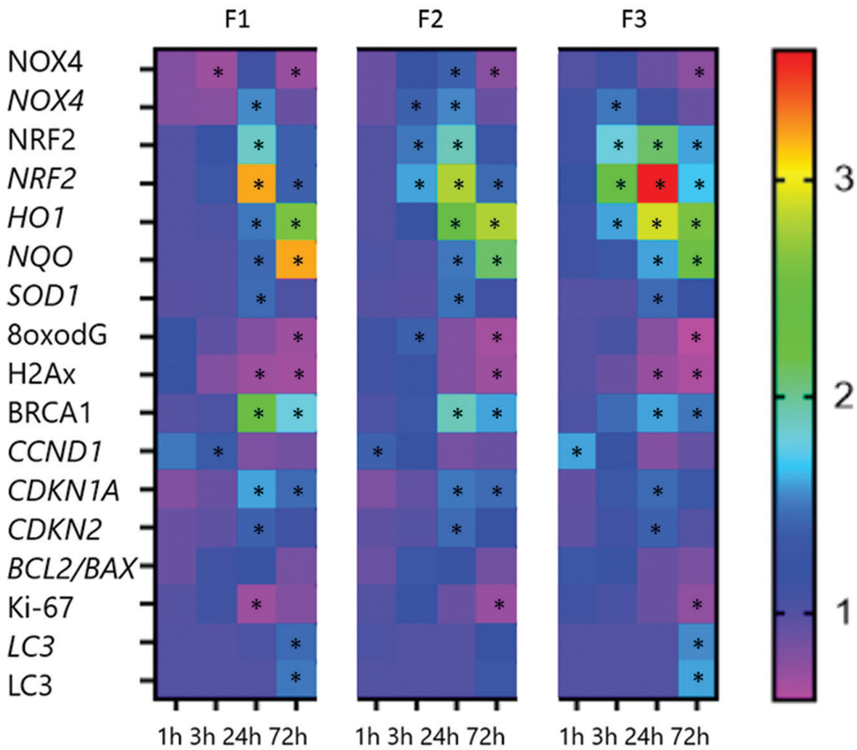

Figure 5. Heat maps of genes and proteins expression in human embryonic lung fibroblasts in response to the incubation with the fullerenes F1, F2 and F3. $^*P < 0.01$, vs. control (non-parametric Mann-Whitney *U* test).
Abbreviations: 8oxodG: 8-oxo-2'-deoxyguanosine; BCL2: B-cell lymphoma 2; BAX: Bcl-2-like protein 4; BRCA1: Breast cancer 1; CCND1: Cyclin D1; CDKN1A: Cyclin-dependent kinase inhibitor 1A; CDKN2: Cyclin-dependent kinase inhibitor 2A; H2Ax: H2A histone family member X; HO1: Heme oxygenase 1; Ki-67: Antigen Kiel 67; LC3: Light chain 3 protein; NOX4: NADPH oxidase 4; NQO1: NAD(P)H quinone dehydrogenase 1; NRF2: Nuclear factor erythroid 2-related factor 2; SOD1: Superoxide dismutase 1.

activate *SOD1* to reduce intracellular ROS. The variations in its expression are less than 50%, which is why we have categorised it as the second group in **Table 2**. The activation of its expression was observed after a period of 24 hours for all derivatives of fullerene.

8OxoG is a result of ROS interaction with DNA, which makes it an efficient marker of DNA oxidative damage.[61] For F1 and F3 we found its decrease after 72 hours. This fact can be explained by our previous data - possibly, activated *NRF2* inhibits ROS that results in 8OxoG decrease. For F2, we observed the same general trend, with the exception of the 3-hour mark, where there is an increase of 8OxoG. It is possible that such an increase is associated with a concurrent rise in the expression of the *NOX4* gene. In general, based on the 8-oxoG marker, there appears to be reduction of oxidative damage to DNA after fullerenes addition to the cells.

In order to investigate the presence of double-strand DNA breaks, we conducted an analysis of the H2AX histone protein that is phosphorylated at the sites of damage.[62] For all of the tested fullerenes, we observed the decreased level of the protein. For F1 and F3 the decreased level was also observed after only 24 hours, for F2 – after 72 hours.

By analysis of *CCND1*, *CDKN1A* and *CDKN2*, we have examined the alterations in the progression of the cell cycle. *CCND1* facilitates the transition of cells from the G1 phase to the S phase, which is a precursor to mitosis.[63] The fullerenes demonstrated the increased level of the gene expression meaning the successful cell cycle progression. F1 and F3 fullerenes produced significant changes and we placed this gene in group 1, when F2 induced weaker changes in its expression and we placed it in group 2 (**Table 2**). As shown in **Figure 5**, *CCND1* expression increased in 1 hour after F2 and F3 addition reflecting the better cells sensitivity to fullerenes with the addends containing longer carbon chain. Compared to F2 and F3, F1 changed *CCND1* gene expression later, only after 3 hours.

CDKN1A coding p21 protein is a cell cycle inhibitor which arrests the cycle progression and inhibits cyclin-dependent kinases.[64] In general, all three fullerenes enhanced the expression level, but the changes were more pronounced for F1 and F2 (**Table 2**). It should be noted that *CCND1* expression changes after 3 hours while *CDKN1A* after 24 and 72 hours (**Figure 5**), therefore the activated life cycle progression in a short-period results in activation of cell arrest in a longer perspective.

CDKN2 is a well-known tumour-suppressing gene inhibiting uncontrolled cellular growth and division.[65] The expression of that gene increased after all fullerenes and because its changes were less than 50% it belongs to the second group (**Table 2**). De facto, CDKN2 becomes activated in concert with CDKN1A following a period of 24 hours, thus they collaborate in halting the progression of the cell cycle. Furthermore, we explored the expression of the *Ki67* gene, as it is also implicated in the processes of mitosis, regulating the formation of mitotic chromosome periphery compartment and preventing their clustering.[66] We have demonstrated a reduction in the level of its expression for all the compounds under investigation, indicating a mitotic inhibition in the cells. The changes occur after 24 or 72 hours and the value of changes corresponds to group 2 (**Table 2**).

Another gene indirectly related to the cell cycle progression and DNA repair is *BRCA1*.[67] It was shown that mutations in that gene result in oncogenic transformation in cells, which cannot repair their genome.[68] This gene expression was significantly activated and it was placed in the first group for all fullerenes (**Table 2**). *BRCA1* gene expression has started after 24 hours and continued until 72 hours (**Figure 5**).

BCL2 is a protein that acts as an apoptosis inhibitor, effectively neutralising the activity of the pro-apoptotic protein BAX.[69-71] The BCL2/BAX balance governs the cell's decision-making process — whether to undergo apoptosis or not. In our experiments, there was no discernible shift towards either an increase or a decrease. Therefore, the outcome indicates a harmonious equilibrium between pro-apoptotic and anti-apoptotic dynamic within the cells.

Autophagy was investigated with *LC3* gene and protein expression. It is worth noting that for the F3 compound, both protein and gene expressions underwent significant alterations and were categorised in the first group (**Table 2**). For F2, the changes in the expression were non-significant. After F1, changes of *LC3* protein expression were more pronounced than of *LC3* gene. Thus, for F1 and F3 we noticed an increase of autophagy meaning that cells utilise some of their damaged or useless organelles to construct the new ones after 72 hours.[72]

4. Discussion

Overall, based on the extensive research, we conclude the antioxidant effect of fullerene derivatives in the following sequence according to their gene/protein expression – F3 < F2 < F1. Fullerene with the greater carbon chain, or F3, demonstrated the rapid activation of the panel of antioxidant factors – *NRF2*, *HO1*, *NQO1*, and *SOD1*. This led to a reduction of the DNA damage markers – 8OxoG and H2AX. The initial stimulation of the cell-division cycle progression by CCND1 only after 1 hour is a signal of suitable conditions for cells division. Later inhibition of the cell cycle by *CDKN1A*, *CDKN2*, *Ki-67* and *BRCA1* is an adequate response to the preliminary activated gene of cell cycle progression devoted to stop cell overgrowth. The delayed induction of autophagy is a mechanism employed by cells to conserve precious resources and restore their structural integrity.

A similar overall pattern was observed for the compound F2, but the level of antioxidant gene activation does not reach the same degree as that observed for F1. For example, *NRF2* and *HO1* expression was lower by 20–30%. Due to the postponed activation of the *NRF2* gene, we positioned F1 at the end of the series of compounds under investigation in terms of their antioxidant capacity.

To recapitulate all the data, a decline in intracellular ROS detected by flow cytometry revealed that the F1 effect was more rapid than the F2 and F3 effects in terms of antioxidant activity (**Figure 2B**). Probably, the observed reduction in intracellular ROS can be attributed to a decrease in the expression of the NOX4 protein (**Figure 5**). Intracellular fluorescence of F1 fullerene has a maximum intensity after 3 hours, but we were not able to register the associated changes in gene/protein expression. It is possible that F1 has been able to capture ROS in the intracellular space. Nonetheless, the results of cytotoxicity assay conducted in the present study revealed a 5-fold increase in the toxicity of compound F1 compared to other two compounds, thus rendering it highly detrimental to cells.

Compounds F2 and F3 are very similar in terms of their biological effects on Human embryonic lung fibroblasts. Their profiles of cytotoxicity and cell viability are very close. For both compounds significant intracellular ROS decrease was determined after 24 hours. A discrepancy in the gene/protein expression patterns was observed between F2 and F3 compounds. In the case of F3, the genes maintained an elevated level of expression even after 72 hours, suggesting a protracted F3 effect. Variability between F2 and F3 was found in gene/protein expressions. In case of F3 the genes continued to have an increased level of expression after 72 hours, so the compound effect is also prolonged.

5. Conclusions

The biological effects of the water-soluble thiophene-based C_{70} fullerene derivatives were extensively studied on human embryo lung fibroblasts. Intracellular oxidative stress, cytotoxicity response and the expression of key genes and proteins were tested to reveal if the compounds have an antioxidant effect. The solubilising addends in the investigated compounds were only different in the length of the aliphatic chain. Nonetheless, this subtle alteration had a profound impact on the antioxidative properties of fullerene derivatives. Thus, we have found that the antioxidant activity of fullerenes can be ranked in descending order of potency based on gene/protein expression, with F3 being the most potent, followed by F2 and then F1. The longer carbon chain resulted in a pronounced antioxidant activity prolonged up to 72 hours. The revealed effect is fundamentally different from the effect of the pristine C_{70} fullerene on cells, which exhibits prooxidant properties. Thus, modification of the surface with substituents that enhance the antioxidant properties of the substance leads to a change in the mechanism of the effect of nanoparticles on the genetic apparatus of the cells. The findings obtained can be utilised in forecasting the anti-oxidative properties of fullerenes, which could contribute to the development of innovative pharmaceuticals for addressing ischemic disorders, stress-induced conditions, age-related issues, and other practical healthcare challenges.

Acknowledgement

None.

Financial support

The synthesis of water-soluble fullerene derivatives was supported by the Russian Science Foundation, project No. 22-43-08005, other research was supported by state assignment of the Ministry of Science and Higher Education.

Conflicts of interest statement

The authors declare no conflict of interest.

Author contributions

Conceptualization: SVK and NV; *Data curation*: MC and PU; *Formal analysis*: ES and VB; *Funding acquisition*: SK and SVK; *Investigation*: EE, LK, and IR; *Methodology*: PT and OK; *Project administration*: SVK; *Resources*: SK; *Supervision*: NV; Software, ES and PU; *Validation*: EP, PU, and SEK; *Visualisation*: TS and VS; *Writing—original draft:* MC; *Writing—review & editing*: PU. All authors have read and agreed to the published version of the manuscript.

Ethics approval and consent to participate

Not applicable.

Consent for publication

Not applicable.

Availability of data

Not applicable.

Open access statement

References

1. Kroto HW, Heath JR, O'Brien SC, Curl RF, Smalley RE. C60: Buckminsterfullerene. *Nature.* 1985;318:162-163. doi: 10.1038/318162a0
2. McNamara K, Tofail SAM. Nanoparticles in biomedical applications. *Adv Phys X.* 2017;2:54-88. doi: 10.1080/23746149.2016.1254570
3. Blum AP, Kammeyer JK, Rush AM, Callmann CE, Hahn ME, Gianneschi NC. Stimuli-responsive nanomaterials for biomedical applications. *J Am Chem Soc.* 2015;137:2140-2154. doi: 10.1021/ja510147n
4. Zhao Y, Zhang Z, Pan Z, Liu Y. Advanced bioactive nanomaterials for biomedical applications. *Exploration (Beijing).* 2021;1:20210089. doi: 10.1002/EXP.20210089
5. Bakry R, Vallant RM, Najam-ul-Haq M, *et al.* Medicinal applications of fullerenes. *Int J Nanomedicine.* 2007;2:639-649.
6. Castro E, Garcia AH, Zavala G, Echegoyen L. Fullerenes in biology and medicine. *J Mater Chem B.* 2017;5:6523-6535. doi: 10.1039/C7TB00855D
7. Yin JJ, Lao F, Fu PP, *et al.* The scavenging of reactive oxygen species and the potential for cell protection by functionalized fullerene materials. *Biomaterials.* 2009;30:611-621. doi: 10.1016/j.biomaterials.2008.09.061
8. Çiçek B, Kenar A, Nazir H. Simultaneous determination of C60 and C70 fullerenes by a spectrophotometric method. *Fullerene Sci Technol.* 2001;9:103-111. doi: 10.1081/FST-100000169
9. Eklund PC, Rao AM, Zhou P, Wang Y, Holden JM. Photochemical transformation of C60 and C70 films. *Thin Solid Films.* 1995;257:185-203. doi: 10.1016/0040-6090(94)05704-4
10. Catalan J, Elguero J. Fluorescence of fullerenes (C60 and C70). *J Am Chem Soc.* 1993;115:9249-9252. doi: 10.1021/ja00073a046
11. Liu J, Huang M, Zhang X, *et al.* Polyoxometalate nanomaterials for enhanced reactive oxygen species theranostics. *Coord Chem Rev.* 2022;472:214785. doi: 10.1016/j.ccr.2022.214785
12. Joorabloo A, Liu T. Recent advances in reactive oxygen species scavenging nanomaterials for wound healing. *Explor (Beijing).* 2024;4:20230066. doi: 10.1002/EXP.20230066
13. Zhou Y, Zhen M, Guan M, *et al.* Amino acid modified [70] fullerene derivatives with high radical scavenging activity as promising bodyguards for chemotherapy protection. *Sci Rep.* 2018;8:16573. doi: 10.1038/s41598-018-34967-7
14. Bannunah AM, Vllasaliu D, Lord J, Stolnik S. Mechanisms of nanoparticle internalization and transport across an intestinal epithelial cell model: Effect of size and surface charge. *Mol Pharm.* 2014;11:4363-4373. doi: 10.1021/mp500439c
15. Kopac T. Protein corona, understanding the nanoparticle-protein interactions and future perspectives: A critical review. *Int J Biol Macromol.* 2021;169:290-301. doi: 10.1016/j.ijbiomac.2020.12.108
16. Kornev AB, Peregudov AS, Martynenko VM, Balzarini J, Hoorelbeke B, Troshin PA. Synthesis and antiviral activity of highly water-soluble polycarboxylic derivatives of [70]fullerene. *Chem Commun (Camb).* 2011;47:8298-8300. doi: 10.1039/c1cc12209f
17. Huang L, Wang M, Sharma SK, *et al.* Decacationic [70]fullerene approach for efficient photokilling of infectious bacteria and cancer cells. *ECS Trans.* 2013;45:10.1149/04520.0065ecst.65 doi: 10.1149/04520.0065ecs
18. Marforio TD, Mattioli EJ, Zerbetto F, Calvaresi M. Fullerenes against COVID-19: Repurposing C_{60} and C_{70} to clog the active site of SARS-CoV-2 protease. *Molecules.* 2022;27:1916. doi: 10.3390/molecules27061916
19. Mikheev IV, Sozarukova MM, Izmailov DY, Kareev IE, Proskurnina EV, Proskurnin MA. Antioxidant potential of aqueous dispersions of fullerenes C_{60}, C_{70}, and Gd@C_{82}. *Int J Mol Sci.* 2021;22:5838. doi: 10.3390/ijms22115838
20. Mikheev IV, Sozarukova MM, Proskurnina EV, Kareev IE, Proskurnin MA. Non-functionalized fullerenes and endofullerenes in aqueous dispersions as superoxide scavengers. *Molecules.* 2020;25:2506. doi: 10.3390/molecules25112506
21. Tzirakis MD, Orfanopoulos M. Radical reactions of fullerenes: From synthetic organic chemistry to materials science and biology. *Chem Rev.* 2013;113:5262-5321. doi: 10.1021/cr300475r
22. Grebowski J, Kazmierska P, Krokosz A. Fullerenols as a new therapeutic approach in nanomedicine. *Biomed Res Int.* 2013;2013:751913. doi: 10.1155/2013/751913
23. Roman G. Thiophene-containing compounds with antimicrobial activity. *Arch Pharm (Weinheim).* 2022;355:e2100462. doi: 10.1002/ardp.202100462
24. Singh A, Singh G, Bedi PMS. Thiophene derivatives: A potent multitargeted pharmacological scaffold. *J Heterocycl Chem.* 2020;57:2658-2703. doi: 10.1002/jhet.3990
25. Mishra R, Sachan N, Kumar N, Mishra I, Chand P. Thiophene scaffold as prospective antimicrobial agent: A review. *J Heterocycl Chem.* 2018;55:2019-2034. doi: 10.1002/jhet.3249
26. Cetin A, Türkan F, Taslimi P, Gulçin İ. Synthesis and characterization of novel substituted thiophene derivatives and discovery of their carbonic anhydrase and acetylcholinesterase inhibition effects. *J Biochem Mol Toxicol.* 2019;33:e22261. doi: 10.1002/jbt.22261
27. Alım Z, Köksal Z, Karaman M. Evaluation of some thiophene-based sulfonamides as potent inhibitors of carbonic anhydrase I and II isoenzymes isolated from human erythrocytes by kinetic and molecular modelling studies. *Pharmacol Rep.* 2020;72:1738-1748. doi: 10.1007/s43440-020-00149-4
28. Xu DG, Lv W, Dai CY, *et al.* 2-(Pro-1-ynyl)-5-(5,6-dihydroxypenta-1,3-diynyl) thiophene induces apoptosis through reactive oxygen species-mediated JNK activation in human colon cancer SW620 cells. *Anat Rec (Hoboken).* 2015;298:376-385. doi: 10.1002/ar.23045
29. Song X, Fanelli MG, Cook JM, Bai F, Parish CA. Mechanisms for the reaction of thiophene and methylthiophene with singlet and triplet molecular oxygen. *J Phys Chem A.* 2012;116:4934-4946. doi: 10.1021/jp301919g
30. Kucur O, Turan HT, Monari A, Aviyente V. Computational study of photo-oxidative degradation mechanisms of boron-containing oligothiophenes. *J Phys Chem A.* 2020;124:1390-1398.

doi: 10.1021/acs.jpca.9b07858

31. Sumita M, Morihashi K. Theoretical study of singlet oxygen molecule generation via an exciplex with valence-excited thiophene. *J Phys Chem A.* 2015;119:876-883. doi: 10.1021/jp5123129
32. Kraevaya OA, Peregudov AS, Fedorova NE, *et al.* Thiophene-based water-soluble fullerene derivatives as highly potent antiherpetic pharmaceuticals. *Org Biomol Chem.* 2020;18:8702-8708. doi: 10.1039/d0ob01826k
33. Kraevaya OA, Peregudov AS, Godovikov IA, *et al.* Direct arylation of $C_{60}Cl_6$ and $C_{70}Cl_8$ with carboxylic acids: A synthetic avenue to water-soluble fullerene derivatives with promising antiviral activity. *Chem Commun (Camb).* 2020;56:1179-1182. doi: 10.1039/c9cc08400b
34. Savinova EA, Salimova TA, Proskurnina EV, *et al.* Effect of water-soluble chlorine-containing buckminsterfullerene derivative on the metabolism of reactive oxygen species in human embryonic lung fibroblasts. *Oxygen.* 2023;3:1-19. doi: 10.3390/oxygen3010001
35. Proskurnina EV, Mikheev IV, Savinova EA, *et al.* Effects of aqueous dispersions of C_{60}, C_{70} and Gd@C_{82} fullerenes on genes involved in oxidative stress and anti-inflammatory pathways. *Int J Mol Sci.* 2021;22:6130. doi: 10.3390/ijms22116130
36. Sergeeva V, Kraevaya O, Ershova E, *et al.* Antioxidant properties of fullerene derivatives depend on their chemical structure: A study of two fullerene derivatives on HELFs. *Oxid Med Cell Longev.* 2019;2019:4398695. doi: 10.1155/2019/4398695
37. Guo J, Zhao Z, Shang ZF, Tang Z, Zhu H, Zhang K. Nanodrugs with intrinsic radioprotective exertion: Turning the double-edged sword into a single-edged knife. *Exploration (Beijing).* 2023;3:20220119. doi: 10.1002/EXP.20220119
38. Huang HJ, Chetyrkina M, Wong CW, *et al.* Identification of potential descriptors of water-soluble fullerene derivatives responsible for antitumor effects on lung cancer cells via QSAR analysis. *Comput Struct Biotechnol J.* 2021;19:812-825. doi: 10.1016/j.csbj.2021.01.012
39. Yang H, Sun L, Li W, Liu G, Tang Y. *In silico* prediction of chemical toxicity for drug design using machine learning methods and structural alerts. *Front Chem.* 2018;6:30. doi: 10.3389/fchem.2018.00030
40. Knyazev VD. Effects of chain length on the rates of C-C bond dissociation in linear alkanes and polyethylene. *J Phys Chem A.* 2007;111:3875-3883. doi: 10.1021/jp066419e
41. Wong-Ekkabut J, Baoukina S, Triampo W, Tang IM, Tieleman DP, Monticelli L. Computer simulation study of fullerene translocation through lipid membranes. *Nat Nanotechnol.* 2008;3:363-368. doi: 10.1038/nnano.2008.130
42. Nalakarn P, Boonnoy P, Nisoh N, Karttunen M, Wong-Ekkabut J. Dependence of fullerene aggregation on lipid saturation due to a balance between entropy and enthalpy. *Sci Rep.* 2019;9:1037. doi: 10.1038/s41598-018-37659-4
43. Thannickal VJ, Fanburg BL. Reactive oxygen species in cell signaling. *Am J Physiol Lung Cell Mol Physiol.* 2000;279:L1005-L1028. doi: 10.1152/ajplung.2000.279.6.L1005
44. D'Autréaux B, Toledano MB. ROS as signalling molecules: Mechanisms that generate specificity in ROS homeostasis. *Nat Rev Mol Cell Biol.* 2007;8:813-824. doi: 10.1038/nrm2256
45. Dröge W. Free radicals in the physiological control of cell function. *Physiol Rev.* 2002;82:47-95. doi: 10.1152/physrev.00018.2001
46. Girard-Lalancette K, Pichette A, Legault J. Sensitive cell-based assay using DCFH oxidation for the determination of pro- and antioxidant properties of compounds and mixtures: Analysis of fruit and vegetable juices. *Food Chem.* 2009;115:720-726. doi: 10.1016/j.foodchem.2008.12.002
47. Markovic Z, Trajkovic V. Biomedical potential of the reactive oxygen species generation and quenching by fullerenes (C60). *Biomaterials.* 2008;29:3561-3573. doi: 10.1016/j.biomaterials.2008.05.005
48. Kong L, Zepp RG. Production and consumption of reactive oxygen species by fullerenes. *Environ Toxicol Chem.* 2012;31:136-143. doi: 10.1002/etc.711
49. De Araújo Neto LN, De Lima M, De Oliveira JF, *et al.* Thiophene-thiosemicarbazone derivative (L10) exerts antifungal activity mediated by oxidative stress and apoptosis in *C. Albicans. Chem Biol Interact.* 2020;320:109028. doi: 10.1016/j.cbi.2020.109028
50. Cai G, Wang S, Zhao L, *et al.* Thiophene derivatives as anticancer agents and their delivery to tumor cells using albumin nanoparticles. *Molecules.* 2019;24:192. doi: 10.3390/molecules24010192
51. Amara N, Goven D, Prost F, Muloway R, Crestani B, Boczkowski J. NOX4/NADPH oxidase expression is increased in pulmonary fibroblasts from patients with idiopathic pulmonary fibrosis and mediates TGFbeta1-induced fibroblast differentiation into myofibroblasts. *Thorax.* 2010;65:733-738. doi: 10.1136/thx.2009.113456
52. Jiang F, Liu GS, Dusting GJ, Chan EC. NADPH oxidase-dependent redox signaling in TGF-β-mediated fibrotic responses. *Redox Biol.* 2014;2:267-272. doi: 10.1016/j.redox.2014.01.012
53. Rojo De La Vega M, Chapman E, Zhang DD. NRF2 and the hallmarks of cancer. *Cancer Cell.* 2018;34:21-43. doi: 10.1016/j.ccell.2018.03.022
54. Ma Q. Role of nrf2 in oxidative stress and toxicity. *Annu Rev Pharmacol Toxicol.* 2013;53:401-426. doi: 10.1146/annurev-pharmtox-011112-140320
55. Smyrnias I, Zhang X, Zhang M, *et al.* Nicotinamide adenine dinucleotide phosphate oxidase-4-dependent upregulation of nuclear factor erythroid-derived 2-like 2 protects the heart during chronic pressure overload. *Hypertension.* 2015;65:547-553. doi: 10.1161/HYPERTENSIONAHA.114.04208
56. Mir S, Ormsbee Golden BD, Griess BJ, *et al.* Upregulation of Nox4 induces a pro-survival Nrf2 response in cancer-associated fibroblasts that promotes tumorigenesis and metastasis in part via Birc5 induction. *Breast Cancer Res.* 2022;24:48. doi: 10.1186/s13058-022-01548-6
57. Lee JM, Johnson JA. An important role of Nrf2-ARE pathway in the cellular defense mechanism. *J Biochem Mol Biol.* 2004;37:139-143. doi: 10.5483/bmbrep.2004.37.2.139
58. Saha S, Buttari B, Panieri E, Profumo E, Saso L. An overview of Nrf2 signaling pathway and its role in inflammation. *Molecules.* 2020;25:5474. doi: 10.3390/molecules25225474
59. Ross D, Siegel D. Functions of NQO1 in cellular protection and Co_{Q10} metabolism and its potential role as a redox sensitive molecular switch. *Front Physiol.* 2017;8:595. doi: 10.3389/fphys.2017.00595
60. Araujo JA, Zhang M, Yin F. Heme oxygenase-1, oxidation, inflammation, and atherosclerosis. *Front Pharmacol.* 2012;3:119. doi: 10.3389/fphar.2012.00119
61. Weimann A, Belling D, Poulsen HE. Quantification of 8-oxo-guanine and guanine as the nucleobase nucleoside and deoxynucleoside forms in human urine by high-performance liquid chromatography-electrospray tandem mass spectrometry. *Nucleic Acids Res.* 2002;30:E7. doi: 10.1093/nar/30.2.e7
62. Collins PL, Purman C, Porter SI, *et al.* DNA double-strand breaks induce H2Ax phosphorylation domains in a contact-dependent manner. *Nat Commun.* 2020;11:3158. doi: 10.1038/s41467-020-16926-x
63. Moreno-Bueno G, Rodríguez-Perales S, Sánchez-Estévez C, *et al.* *Cyclin D1* gene (*CCND1*) mutations in endometrial cancer. *Oncogene.* 2003;22:6115-6118. doi: 10.1038/sj.onc.1206868
64. Cazzalini O, Scovassi AI, Savio M, Stivala LA, Prosperi E. Multiple roles of the cell cycle inhibitor p21(CDKN1A) in the DNA damage response. *Mutat Res.* 2010;704:12-20.

doi: 10.1016/j.mrrev.2010.01.009
65. Liang J, Fan J, Wang M, *et al*. CDKN2A inhibits formation of homotypic cell-in-cell structures. *Oncogenesis.* 2018;7:50. doi: 10.1038/s41389-018-0056-4
66. Uxa S, Castillo-Binder P, Kohler R, Stangner K, Müller GA, Engeland K. *Ki-67* gene expression. *Cell Death Differ*. 2021;28:3357-3370. doi: 10.1038/s41418-021-00823-x
67. Roy R, Chun J, Powell SN. BRCA1 and BRCA2: Different roles in a common pathway of genome protection. *Nat Rev Cancer*. 2011;12:68-78. doi: 10.1038/nrc3181
68. Gorodetska I, Kozeretska I, Dubrovska A. *BRCA* genes: The role in genome stability, cancer stemness and therapy resistance. *J Cancer*. 2019;10:2109-2127. doi: 10.7150/jca.30410
69. Tzifi F, Economopoulou C, Gourgiotis D, Ardavanis A, Papageorgiou S, Scorilas A. The role of BCL2 family of apoptosis regulator proteins in acute and chronic leukemias. *Adv Hematol.* 2012;2012:524308. doi: 10.1155/2012/524308
70. Hardwick JM, Soane L. Multiple functions of BCL-2 family proteins. *Cold Spring Harb Perspect Biol.* 2013;5:a008722. doi: 10.1101/cshperspect.a008722
71. Gross A, Katz SG. Non-apoptotic functions of BCL-2 family proteins. *Cell Death Differ*. 2017;24:1348-1358. doi: 10.1038/cdd.2017.22
72. Klionsky DJ. Autophagy: From phenomenology to molecular understanding in less than a decade. *Nat Rev Mol Cell Biol.* 2007;8:931-937. doi: 10.1038/nrm2245

Received: September 29, 2024
Revised: November 18, 2024
Accepted: December 31, 2024
Available online: September 22, 2025